Proceedings of ASME Turbo Expo 2017: Turbomachinery Technical Conference and Exposition
GT2017
June 26-30, 2017, Charlotte, NC, USA

GT2017-65242

Real-Time Fuel Cell Model Development Challenges for Cyber-Physical Systems in Hybrid Power Applications

David Tucker
U.S. Department of Energy
National Energy Technology Laboratory
3610 Collins Ferry Road
Morgantown, WV 26507-0880

Nor Farida Harun*, Valentina Zaccaria*
U.S. Department of Energy
National Energy Technology Laboratory
3610 Collins Ferry Road
Morgantown, WV 26507-0880

Kenneth M. Bryden
Simulation and Decision Science Program,
Ames Laboratory U.S. Department of Energy,
Ames, IA USA

Comas Haynes
Georgia Tech Research Institute/Oak Ridge
National Laboratory
Atlanta, GA, USA /Oak Ridge, TN, USA

ABSTRACT

The use of cyber-physical systems to simulate novel hybrid power cycles provides a cost-effective means to develop and test control strategies at the pilot scale. One of the primary challenges of implementing a cyber-physical power system component is the seamless coupling of a real-time model with hardware that interacts with its environment. A real-time solid oxide fuel cell model integrated with a physical recuperated turbine cycle results in significant capability in exploring the operational limits of a hybrid system. The creation of a model that can interact with hardware requires a delicate balancing act between fidelity, speed, and stability. In this case, the developed model makes use of both implicit and explicit methods for solving the differential equations associated with heat transfer and electrochemistry in a solid oxide fuel cell system. Stability and computational speed are evaluated over some transient simulations. The balance between implicit and explicit methodologies for solving the differential equations associated with heat transfer and the temperature profiles was examined. The method is particularly relevant during simulations involving localized degradation distributed along the cell. The results provide some quantification of the challenges faced in applying cyber-physical systems to hardware simulation of advanced power systems.

Keywords: Cyber-Physical System, Real-Time Model, Solid Oxide Fuel Cell, Gas Turbine, Hybrid Power, Degradation

INTRODUCTION

Stemming from embedded systems, cyber-physical systems have found applications in autonomous robots and vehicles [1-3]. They are expected to play a critical role also in the future of distributed energy, in terms of control of smart grids [1, 4]. Cyber-physical systems are also being pursued to replace the irreplaceable in biological applications such as the development of an artificial heart [5]. Another form/application of cyber-physical systems is to mimic the behavior of something that doesn't exist…yet. This would provide tremendous insight into the nature of such developing technology, and provide a means for ensuring the final product will meet the performance targets required for commercialization at a fraction of the cost of pilot studies.

As an example, solid oxide fuel cells (SOFCs), capable of being integrated into a power cycle with a gas turbine because of their high operating temperatures, represent the promise of extremely high efficiency and the lowest possible emissions [6-8]. There have been numerous SOFC products tested in the marketplace as stand-alone devices, but limited demonstrations of the technology in a pressurized environment fully coupled to a turbine [9-11]. The main reason for such limited demonstration of this hybrid technology is the cost associated with pilot, or even sub-pilot fuel cell system.

*This work was done under the U.S. Department of Energy (DOE) Postgraduate and Graduate Research Program at the National Energy Technology Laboratory (NETL), managed by the Oak Ridge Institute for Science and Education (ORISE)

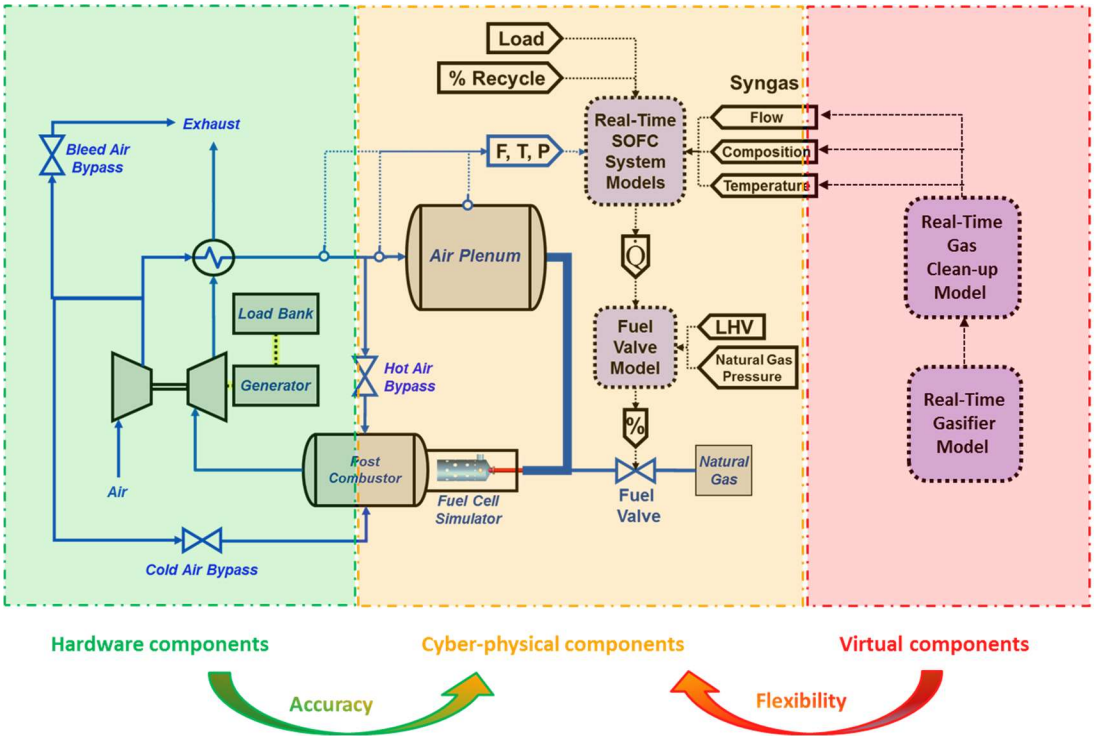

Figure 1
Layout of the Hybrid Performance Project Facility at NETL Illustrating the Connectivity of the Cyber-Physical Fuel Cell System and Real-Time Model

An approach to explore the capabilities of this technology taken by the National Energy Technology Laboratory (NETL) was to build a cyber-physical fuel cell system at meaningful scale (200 kW to 600 kW) that could be coupled to a physical gas turbine and exhaust gas recuperators and virtually coupled to a numeric representation of gasifier and fuel processing equipment [12, 13]. Through a collaboration between NETL and Ames Laboratory (Ames), control strategies were developed for these systems that led to tremendous system flexibility and ultimately to consideration of redesigning the fuel cell system in order to improve economic viability and deal with issues facing the modern grid [14, 15]. A diagram of the layout is shown in Figure 1.

The reconfigurable essence of the cyber-physical fuel cell facilitated redesign of the fuel cell in the hybrid configuration without the expense of building another 350 kW fuel cell stack. At the heart of a reconfigurable cyber-physical fuel cell is the real time model that drives the hardware coupled to the gas turbine cycle [13]. A basic diagram of the cyber-physical fuel cell system and its interaction with its environment, both physical and virtual, is shown in Figure 2.

As illustrated in Figure 2, the cyber-physical fuel cell must consider many interactions. In particular, the interactions between computational and physical components present many challenges [16, 17]. As such, the implementation of a cyber-physical system demands changes in both dynamics modeling and computational theory [17, 18]. The requirement of "real-time" requires a careful evaluation of the physics, controller sampling rate, sensor response, actuator performance, interface requirements, and desired diagnostic capabilities [3].

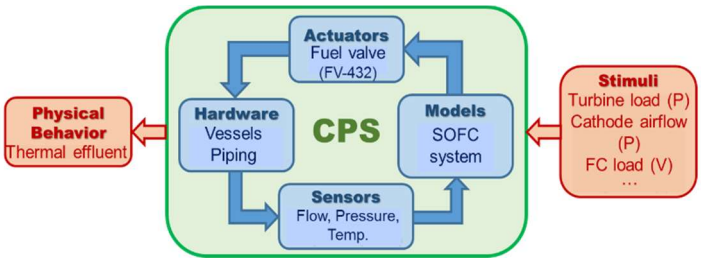

Figure 2
Cyber-Physical Fuel Cell Diagram

This paper provides an evaluation of these parameters as applied to the cyber-physical fuel cell used in the Hybrid Performance (Hyper) project facility at NETL shown in Figure 1, but a similar approach would be required for any cyber-physical system used in technology development. The electrochemical phenomena mimicked by the real-time model to complete all its calculations from sensor inputs in a millisecond time frame. The requirements of distributed, 1D calculations in milliseconds are explored in this paper.

REQUIREMENTS

The first step in designing the dynamic real-time fuel cell model was outlining the requirements for hardware-based simulation in a hybrid configuration. The main goal of the Hyper project focused on controls development and system operability as well as fuel cell failure analysis.

Lumped vs. Distributed

A lumped parameter or zero-dimensional (0D) fuel cell model was first considered for implementation for a cyber-physical system. This had the advantage of speed over a one dimensional (1D) or distributed approach, but diagnostic capability was severely limited. In particular, failure analysis was difficult because only the inlet and outlet conditions could be determined. Solid temperature, for example, was assumed to be linearly distributed between the inlet and the outlet. However, higher order models used in the literature showed steady state profiles with excessive localized temperature gradients, especially with methane rich fuels. During transient operation, non-linear temperature profiles were also observed.

Typical temperature profiles for methane rich fuel and transient operation are compared against the linear case for the same overall inlet to outlet change in temperature in Figure 3 for illustration. It was determined that controls development and adequate failure analysis demanded a higher order model, and so a distributed 1D model was developed.

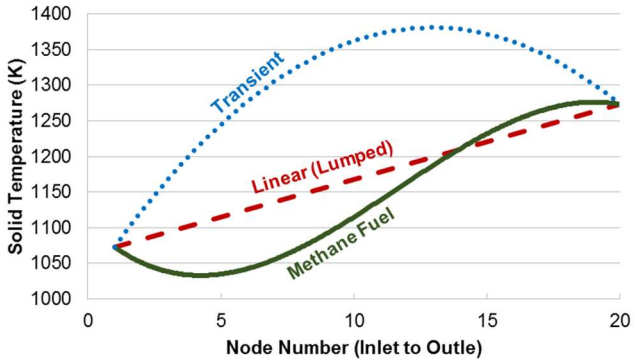

Figure 3
Assumed Linear Temperature Profile of a Lumped Model Compared to 1D Profiles of a Methane Rich Fuel Case and a Transient Behavior Case

Sampling Time

The sampling time must be chosen such that the computational time is always less. However, the sampling time must also be relevant to the environment it is interacting with. This comes down to a compromise with the computational platform and modeling approximations used to accelerate the calculation process.

Some of the more important time scales are provided below in Table 1. The industrial control platform used by the Hyper project facility has a 5 ms time step capability. This correlates with the limitation of the fuel valve used for emulating the thermal effluent of the fuel cell, which makes use of a needle valve with a stepper motor capable of adjustment representative of 20% of full scale in 5 ms steps. Receiving commands from the real-time fuel cell model in a feed-forward manner, 5 ms represents the physical limitation of the hardware to respond to changes in the model.

Table 1- Time Scales Relevant to the Hybrid System

Time Scale	Process
5 µs	Response of power electronics to grid variations
5 ms	Electrochemical response to load variations
5 ms	Control system limitation
5 ms	CPS fuel valve response limitation (20% full scale)
5 ms	Hot wire anemometer flow measurement response
5 ms	Turbine rotational speed measurement response
20 ms	Electrochemical response to composition variations
100 ms	Thermal variations to the turbine from the fuel cell
100 ms	Turbine speed change on thermal or flow variation
150 ms	Pressure transducer response
200 ms	Fastest air valve response (15% of full scale)
400 ms	Anubar flow measurement response
500 ms	Heat transfer in fuel cell or recuperators
500 ms	Thermocouple or thermistor response

In looking at Table 1, it is clear that a 5 ms sampling time would capture all of the relevant dynamics of the system. The dynamics of the power electronics in the microsecond range are generally three orders of magnitude faster than process dynamics relevant to component coupling and control, and so it is assumed that these interactions can be neglected [19, 20].

In testing with a lumped parameter fuel cell model operating embedded in the control platform itself, it was possible to realize the 5 ms sampling time, but the advantages of such speed did not offset the need for distributed diagnostic information during transient operation. Most of the physical processes with impacts on component coupling and control have time scales greater than 100 ms, and so the target of the dynamic real-time model would be a sampling time of less than 100 ms.

The 100 ms sampling time would accommodate failure analysis and relevant time scales for fuel cell failure. These generally occur due to thermal processes like thermally induced stress or delamination, and a 100 ms sampling time is generally sufficient to capture these events in a diagnostic environment.

MODEL DEVELOPMENT

The details of the model developed for the CPS fuel cell in the Hyper facility have been published previously [13]. The technology simulated includes a planar, anode-supported, and

co-flow SOFC system with 441 stainless steel interconnects, a nickel-doped yttria-stabilized zirconia (Ni-YSZ) anode and YSZ electrolyte, and a lanthanum strontium magnetite (LSM) cathode. The dimensions of the channels were designed to be variable, but a channel size of 2mm x 2mm x 20cm was used as a default. Twenty nodes were selected to optimize the balance between the accuracy and the measurement speed at acceptable computational time as suggested in sensitivity analyses [21]. In all cases, a temperature range limitation of 300 K to 1800 K was assumed. To simulate the SOFC with a sampling time less than 100 ms, a number of other simplifications were required.

Electrochemistry

The electrochemical reactions were set up with algebraic relations or such that a finite volume approach could be used for solving the equations without significant computational burden. To accomplish this, only H_2 oxidation was considered in the electrochemical activity. Direct electrochemical oxidation of CO and CH4 were neglected, considering their slower kinetics and the limited electrochemical active area available. This assumption loses validity at higher operating temperatures in excess of 1223K. With this assumption, the Nernst Equation can be simplified to Equation 1, and cell voltage can be calculated by simply subtracting the polarizations, as shown in Equation 2, where η_{dif}, η_{act}, and η_{ohm} are the diffusion, activation, and ohmic polarizations respectively.

$$V_{Nernst} = -\frac{\Delta G^{o}_{H_2O}}{2F} + \frac{R_u T}{2F} \ln\left(\frac{p_{H_2} p_{O_2}^{\frac{1}{2}}}{p_{H_2O}} \right) \quad (1)$$

$$V_{cell} = V_{Nernst} - \eta_{dif} - \eta_{act} - \eta_{ohm} \quad (2)$$

Methane is handled using first order steam reforming kinetics outlined by Achenbach for planar SOFC systems, and the water gas shift reaction is assumed to be in equilibrium [22]. Pressure loss along the cell and the accompanying perfomance degradation was not considered. Pressure loss along the cell was assumed to be negligable. This should be a valid assumption for most cases in the hybrid configuration, where the airflow range is limited in magnitude. Details regarding the approach taken and specific equations for calculation of the polarizations can be found elsewhere [13].

Combustion and Sensible Heat in the Gas Phase

Because the ultimate goal of the model is to provide a feed-forward thermal effluent of the fuel cell post combustor at each time step, gibbs minimization was not required to obtain combustion temperatures. The thermal effluent or $\dot{Q}$, as shown in Figure 1, is calculated as the difference between the sensible heat of the cathode inlet air and the fuel cell post combustor exhaust routed to the turbine.

Because combustion temperatures in the fuel cell system are sufficiently low, below 1400 K, dissociation was neglected and enthalpy calculations were used.

Temperature-dependent specific heat capacity expressions in the gas phase were developed using NASA/Chemkin Polynomials [23]. To further avoid iteration in oxidation calculations, second order polynomials were fit to the higher order polynomials of the Chemkin database over the limited temperature range of fuel cell operation (300 K to 1800 K), and then solved explicitly. A similar approach was taken with other thermophysical properties.

Since the CPS simulation makes use of hardware, heat loss to the environment was not considered. This was physically represented in the hardware, and consideration in the model would double count this effect.

Thermal Performance

The temperature profile in the 1D fuel cell model was calculated using Equation 3, where the second derivative term represents the change in heat flow. Heat transfer mechanisms considered in the model were conductive heat transfer in solid materials, convective heat transfer between solid components and gas stream in the system, and heat generation resulting from electrochemical reaction, water-gas shift, and steam methane reforming, summarized in Equations 3 and 4. The temperature for both solid and gas is calculated at each node. Mass flow is also calculated at each node since the rate of exchange between the anode and cathode is dependent on current density at each time step. The HG_{cell} term in Equation 5 represents the heat generated during electrochemical reactions in the cell; heat generated by steam reforming and water gas shift reactions is shown in Equations 6 and 7, respectively.

$$kA_{channel}\frac{\partial^2 T}{\partial x^2} + hP_g(T_\infty - T) + q_{gen} = \rho c_p \frac{\partial T}{\partial t} \quad (3)$$

$$q_{gen} = HG_{cell} + HG_{WGS} + HG_{SMR} \quad (4)$$

$$HG_{cell} = i\left(\frac{-\Delta H_{H2Oformation}}{2F} - V\right) \quad (5)$$

$$HG_{WGS} = -\Delta n_{CO}\Delta H_{WGS} \quad (6)$$

$$HG_{SMR} = -\Delta n_{CH4}\Delta H_{SMR} \quad (7)$$

Equation 8 shows a detailed expression of Equation 3, considering a fractional weighting factor of β between implicit and explicit formulation for more simulation flexibility. The subscript *i* in Equation 5 refers to the node, while superscript *n* refers to the time step.

$$\begin{aligned} &\beta\left[\frac{kA_s}{(\Delta x)^2}\left(T_{i+1}^{n+1} - 2T_i^{n+1} + T_{i-1}^{n+1}\right) + hP\left(T_\infty - T_i^{n+1}\right)\right] \\ &+(1-\beta)\left[\frac{kA_s}{(\Delta x)^2}\left(T_{i+1}^{n} - 2T_i^{n} + T_{i-1}^{n}\right) + hP_g\left(T_\infty - T_i^{n}\right)\right] \\ &+q_{gen}A_c = \rho C_P\left[\frac{T_i^{n+1} - T_i^{n}}{\Delta t}\right] \end{aligned} \quad (8)$$

Balance between Implicit and Explicit Model

With the explicit method, the solution in each node at the future time step is calculated only from the values at the current time step, thus, no iterations are needed. In contrast, with the implicit scheme, the value at the future time step is present at both sides of the equation. A linear system must be solved for all the nodes at the same time. Therefore, an iterative algorithm is necessary. In particular, in the model used in this work, a tri-diagonal matrix algorithm is employed. Iterations add generally more computational time, making the implicit scheme more complex to implement and more expensive in terms of calculation time. However, implicit methods are usually more stable than explicit ones.

To achieve stability during an explicit calculation, the maximum allowable time step for stability must be less than $0.5\Delta x^2/k$, otherwise the information wouldn't have time to propagate to the next node. Hence, explicit methods are conditionally stable, while implicit methods give a stable solution for bigger time steps. For this reason, although implicit schemes need iterations to be solved and seem more computationally expensive, the possibility to increase the sample time is beneficial to reduce the computational time.

On the other hand, increasing the step size can lead to inaccuracy in the transient behavior of the solution. As a general rule, transient accuracy is ensured only if the iterative scheme converges to a solution of the nonlinear difference equations at each time step. Implicit methods are more efficient when the step size can be increased beyond the explicit stability method because the important time scales of the flow are relatively large such that even large step size gives a good solution.

Summary of Simplifications

The simplifications required to enable a cyber-physical simulation of a fuel cell in the Hyper facility at NETL included:

1. Explicit and implicit finite difference method were applied to evaluate temperature and heat generation distribution across the fuel cell length,
2. Finite volume method was implemented to determine distributed electrochemical properties,
3. Heat loss to the surrounding was neglected in the model because this would be attributed to hardware systems,
4. The SOFC performance was predicted at a single cell level. Thus, the total stack performance was defined as a function of number of cells in the SOFC stack.
5. A temperature range of 300 K to 1800 K was selected to estimate the temperature-dependent thermophysical properties of each material used in the model.
6. A 20 cm fuel cell length was discretized into 20 local positions or nodes with 1 cm each.
7. Only H_2 oxidation was considered in the electrochemical activity. Direct electrochemical oxidation of CO and CH_4 were neglected, considering their slower kinetics and limited electrochemical active area.
8. The effects of pressure loss across the fuel cell length was not included in the model.
9. Second order polynomials were fit to specific heat capacity functions to simplify temperature calculations in the gas phase.
10. Dissociation in combustion was neglected due to the lower operating temperatures of an SOFC.

Test Cases for Thermal Performance

To get a better feel for the potential impact of implicit vs. explicit calculation methods, some test cases were run using the model for sensitivity to the β parameter in Equation 8.

Beta value versus sample time

In order to have a stable solution, the maximum step size required for the explicit method was found to be around 2.5ms. The computational time in that case was fairly independent on β value, varying between 630 and 635 milliseconds.

Increasing the sample time beyond 2.5ms, a fully explicit scheme (β = 0), did not provide a stable solution. For sample time of 40ms and above, only fully implicit schemes were observed to be stable (β = 0.5 and greater). Although temperature changes are normally thought to occur slowly, the mass flow from the cathode to the anode proceeds with changes in the current density, which is affected in milliseconds. This change in mass flow and the associated chemical reactions strongly influences the cell and gas temperature. It is likely that this contributes to instabilities.

Step size and computational time as a function of β

The calculation time required for various values of β at a 5ms sample time is shown in Figure 4. The calculation times were all much greater than 5ms, indicating the need to improve processor speed by two orders of magnitude to realize a 5ms time step with the current model. Solutions below a value of β = 0.2 were not stable.

Similar results are shown for conditions where the sample time was increase to 40ms and 80ms in Figure 5. In these cases, the calculation starts to become unstable for values of β less than 0.5. As shown in the figure, a calculation time 50ms is required at a 40ms sample time, suggesting that a moderate improvement in processor speed would facilitate this sample time. For example, a 40ms sample time can be used on the Hyper project using the dSpace processer, operating at a much higher speed, because the calculation times are all below 30ms.

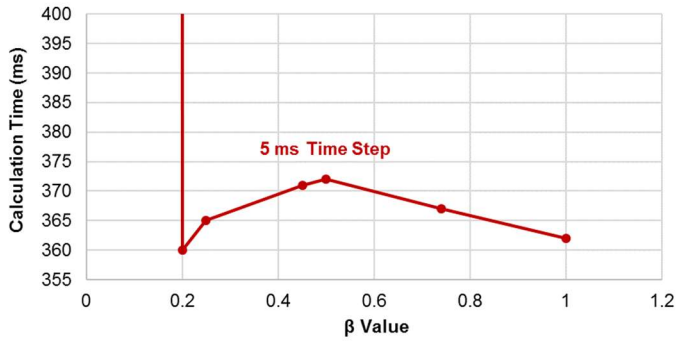

Figure 4
Calculation Time Required as a Function of β for a 5ms Sample Time

However, at a time step of 80ms, the computational time drops even further for implicit solutions, down to 20ms. Since the target for simulations is less than 100ms, most cases are run using an 80ms sample time.

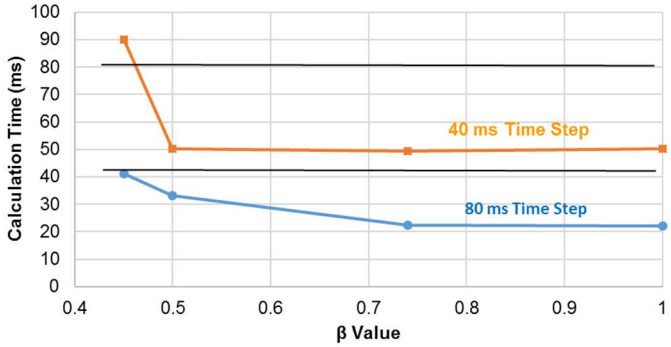

Figure 5
Calculation Time Required as a Function of β for 40ms and 80ms Sample Times

Using a 5ms sample time, the model was used to simulate a change in current load on the fuel cell. The results are shown in Figure 6. Although the optimal computational time was seen at a β value of 0.2, the results start to deviate for values of β below 0.3.

A similar analysis was completed for a sample time of 80ms. In this case, Figure 7 shows a more substantial deviation as the β value drops below 0.5. For β values at or above 0.5, the fully implicit regime, the dynamic simulations produce identical results.

An examination of the average gas temperature calculation shown in Figure 8 reveals the numeric instability associated with the calculation for values of β below 0.5. Clearly, when the results deviate by more than 500 K, the explicit regime must be avoided.

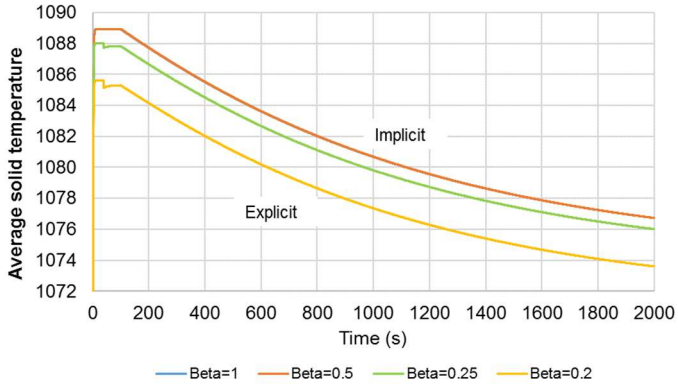

Figure 6
Transient Performance of Average Solid Fuel Cell Temperature during a Current Demand Change for Various Values of β using a 5ms Sample Time

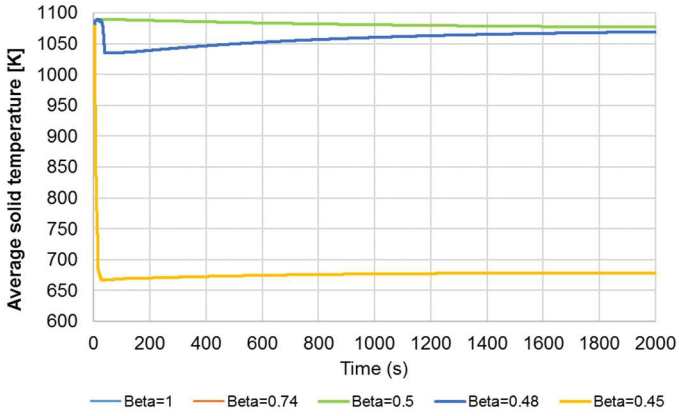

Figure 7
Transient Performance of Average Solid Fuel Cell Temperature during a Current Demand Change for Various Values of β using a 80ms Sample Time

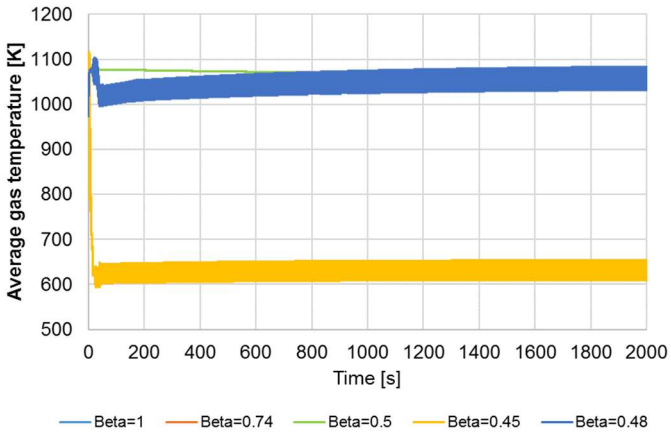

Figure 8
Transient Performance of Average Gas Temperature in the Fuel Cell during a Current Demand Change for Various Values of β using a 80ms Sample Time

It should be noted that any instabilities arising in the fuel cell stack calculation are propagated through other virtual components or sub-components. The selection of the β value must be carefully considered in any real-time model development for cyber-physical systems.

CONCLUSIONS

In the design of cyber-physical systems for technology development, dynamic real-time model development for interaction with hardware is paramount. Meeting the real-time requirement, where computational time is less than the relevant sample time, involves strategies for simplification that can be complex and place restriction on viable operating space. When considering the balance between implicit and explicit calculation methods for heat transfer, instabilities must be avoided.

Reducing the sample time would enable an explicit approach to solving the differential equations associated with heat transfer, however, the real-time calculation requirement could not be maintained. Therefore, an implicit method was required to meet the real-time constraint of the distributed model.

DISCLAIMER

ACKNOWLEDGMENT

This work was funded by the U.S Department of Energy Crosscutting Research program, implemented through the Technology Development & Integration Center, Coal, in The Office of Fossil Energy.

NOMENCLATURE

SOFC	Solid oxide fuel cell
GT	Gas turbine
NETL	National Energy Technology Laboratory
SMR	Steam methane reforming
WGS	Water-gas shift
LHV	Low heating value [kW]
TPB	Triple-phase boundary
Q	Fuel cell waste heat/fuel cell net thermal effluent [kW]
V_{Nernst}	Nernst potential [V]
$\Delta G^{\circ}_{H_2O}$	Standard Gibbs free energy [kJ]
F	Faraday's constant [C/mol]
R_u	Ideal gas constant [J/mol-K]
T	Temperature [K]
P	Gas perimeter [m]
p	Partial pressure [atm]
α	charge transfer coefficient
A	area [m2]
c_p	specific heat [J/kg·K]
h	specific enthalpy variation from reference condition (298 K) [kJ/kg]
h	convective heat transfer coefficient [W/m^{2}K]
HG	heat generation
i	current density [A/cm^2]
i_0	exchange current density [A/cm^2]
k	thermal conductivity [W/m·K]
L	fuel cell length [m]
n	number of electrons transfer per reaction
p	partial pressure [atm]
q_{gen}	specific generated heat [W/m]
r	internal rate
T	temperature [K] or [°C]
V	voltage, overpotential [V]
x	molar fraction
ρ	density [kg/m3]
act	activation
dif	diffusion
ohm	ohmic
$bulk$	anode/cathode stream

REFERENCES

[1] R. Baheti and H. Gill, “Cyber-Physical Systems”, From: “The Impact of Control Technology”, T. Samad and A.M. Annaswamy (eds.), 2011. Available at www.ieeecss.org.

[2] J.M. Bradley, and E.M. Atkins, “Optimization and Control of Cyber-Physical Vehicle Systems,” Sensors 15 (2015) 23020-23049; doi:10.3390/s150923020.

[3] E. A. Lee, "Cyber Physical Systems: Design Challenges," Object Oriented Real-Time Distributed Computing (ISORC), 2008 11th IEEE International Symposium on 5-7 May, 2008, pp. 363-369, DOI 10.1109/ISORC.2008.1, Orlando, FL.

[4] S.K. Khaitan, J.D. McCalley, “Cyber physical system approach for design of power grids: A survey,” Power and Energy Society General Meeting (PES), 2013 IEEE, DOI: 10.1109/PESMG.2013.6672537.

[5] Z. Jiang, M. Pajic, R. Mangharam, “Cyber-Physical Modeling of Implantable Cardiac Medical Devices,” Proceedings of IEEE 2011.

[6] S.K. Park, J.H. Ahn, T.S. Kim, “Performance evaluation of integrated gasification solid oxide fuel cell/gas turbine systems including carbon dioxide capture,” Applied Energy 88 (2011) 2976–2987, doi:10.1016/j.apenergy.2011.03.031.

[7] J. VanOsdol, R. Gemmen, E. Liese, “Examination of the Effect of System Pressure Ratio and Heat Recuperation on the Efficiency of a Coal-Based Gas Turbine Fuel Cell Hybrid Power Generation System With CO_2 Capture,” Journal of Fuel Cell Science and Technology 8 (2011) 041009, DOI: 10.1115/1.4002793.

[8] Diamantis P. Bakalis, Anastassios G. Stamatis, “Incorporating available micro gas turbines and fuel cell: Matching considerations and performance evaluation,” Applied Energy 103 (2013) 607–617, doi: 10.1016/j.apenergy.2012.10.026.

[9] W. Winkler, P. Nehter, M. C. Williams, D. Tucker, R. Gemmen, “General fuel cell hybrid synergies and hybrid system testing status,” J Power Sources 2006;159:656-666.

[10] T.A Adams II, J. Nease, D. Tucker, P. I Barton. Energy conversion with solid oxide fuel cell systems: A review of concepts and outlooks for the short- and long-term. Ind Eng Chem Res 2013;52:3089-3111.

[11] U.S. Department of Energy Fue Cell Technologies Office, Pacific Northwest National Laboratory, “Pathways to Commercial Success: Technologies and Products Supported by the Fuel Cell Technologies Office,” PNNL-22832, September 2013.

[12] D. Tucker, M. Shelton, A.Manivannan, "The Role of Solid Oxide Fuel Cells in Advanced Hybrid Power Systems of the Future," The Electrochemical Society Interface, The Electrochemical Society 2009.

[13] D. Hughes, W. J. Wepfer, K. Davies, J. C. Ford, C. Haynes, , and D. Tucker, "A Real-time Spatial SOFC Model for Hardware-Based Simulation of Hybrid Systems," Proc. ASME 2011 9th International Conference on Fuel Cell Science, Engineering and Technology collocated with ASME 2011 5th International Conference on Energy Sustainability, pp. 409-428.

[14] P. Pezzini, D. Tucker, A. Traverso, “Avoiding Compressor Surge during Emergency Shut-Down Hybrid Turbine Systems,” ASME J. Gas Turbines Power 2013, 135(10), pp. 102602-102602-10.

[15] P. Pezzini, D. Tucker, K. M. Bryden, “Multi-input Single-output Control Strategy for Gas Turbine Hybrids,” Proc. of the 57th Annual ISA Power Industry Division Symposium, June 2016, North Caroline, USA.

[16] P. Derler, E. A. Lee, A. Sangiovanni-Vincentelli. “Modeling Cyber-Physical Systems,” Proceedings of the IEEE (special issue on CPS), 100(1):13-28, January 2012.

[17] A. Rajhans, S.W. Cheng, B. Schmerl, B.H. Krogh, C. Aghi, and A. Bhave, “An Architectural Approach to the Design and Analysis of Cyber-Physical Systems,” Third International Workshop on Multi-Paradigm Modeling, Denver, CO, October 2009.

[18] E. A. Lee, “CPS Foundations” in Proceedings of Design Automation Conference (DAC), ACM, 2010.

[19] K. Schoder, , Z. Cai, S. Sundararajan, M. Yu, M. Sloderbeck, I. Leonard, M. Steurer, “Real-Time Simulation of Communications and Power Systems for Testing Distributed Embedded Controls,” IET Engineering & Technology Reference 2016, 9 pp. doi:10.1049/etr.2015.0022.

[20] G. F. Lauss, M. O. Faruque, K. Schoder, C. Dufour, A. Viehweider, J. Langston, “Characteristics and Design of Power Hardware-in-the-Loop Simulations for Electrical Power Systems,” IEEE Transactions on Industrial Electronics 2016, 63(1), 406-417. doi:10.1109/TIE.2015.2464308.

[21] D. F. Cheddie, N. D. H. Munroe, "A dynamic 1D model of a solid oxide fuel cell for real time simulation," Journal of Power Sources 2007, 171(2), pp. 634-643.

[22] Achenbach, E., “Three-Dimensional and Time-Dependent Simulation of a Planar Solid Oxide Fuel Cell Stack,” Journal of Power Sources, 1994. 49: p. 333-348.

[23] R. J. Kee, F. M. Rupley, and J. A. Miller, "The Chemkin Thermodynamic Data Base" Sandia National Laboratories Report SAND87-8215B (1990).